Proceedings of the 16th International Heat Transfer Conference, IHTC-16
August 10–15, 2018, Beijing, China

IHTC16-23612

SOME ASPECTS OF PRESUMED FILTERED DENSITY FUNCTIONS FORMULATION IN THE CONTEXT OF LARGE EDDY SIMULATION OF TURBULENT REACTING FLOWS

V. Stetsyuk,[1,*] K. Kubiak,[1] L. Liu,[2] J. C. Chai[1]

[1]School of Computing and Engineering, University of Huddersfield, Huddersfield, HD1 3DH, UK
[2]School of Applied Sciences, University of Huddersfield, Huddersfield, HD1 3DH, UK

ABSTRACT

In Large Eddy Simulations (LES) of turbulent flows, spatially-averaged versions of the Navier-Stokes equations are solved on a grid, which is coarse relative to the smallest turbulent length scales [1]. In order to couple the detailed chemistry and the computed flow field in LES of reacting flows, the so-called filtered density function-based approach for subfilter-scale modelling was suggested [2]. This approach was named as the laminar flamelet and allowed to link the complex chemistry to a single variable, i.e. mixture fraction. The mixture fraction is obtained by the solution of corresponding filtered transport equation and subgrid-scale (SGS) variance (the residual field) is usually modelled [3]. The objective of this article is to present in-depth analysis of filtered density functions (FDFs) by analysing experimental data obtained from two-dimensional planar, laser induced fluorescence measurements in isothermal swirling coaxial turbulent jets at a constant Reynolds number of 29000. The FDFs were analysed as a function of flow swirl number, spatial locations in the flow and were linked to the measured subgrid scale variance. In addition, presumed FDFs were also analysed and associated laminar flamelet solution integration errors were evaluated. It was experimentally found that the FDFs can become unimodal when SGS variance reaches a certain value. However, bimodal FDFs were observed in flow regions with high SGS variance. It was demonstrated that bimodality does not automatically result in large errors in resolved variables when top-hat FDF or -FDF formulations are used. It was suggested that possible source of errors in resolved variables could be linked to the SGS variance models rather than to the presumed FDF-based models.

KEY WORDS: Presumed filtered functions; Reacting flows; LES; Measurements, LIF

1. INTRODUCTION

In large eddy simulation (LES) method, spatially-averaged version of the Navier-Stokes equations are solved on a grid, which is relatively coarse with respect to the smallest structures of the flow. The LES method explicitly computes large-scale and time dependent flow features while, small and isotropic structures (subgrid scale) are modelled. Therefore, the LES method captures low-frequency variations of all flow variables, e.g. temperature, mixture fraction, velocity and etc. In the context of LES method, any spatially-averaged (filtered variable) can be computed as a convolution of original non-filtered field with a convolution kernel as, where the filter function acts as a low-pass filter $\bar{f}(x,t) = \int_{-\infty}^{+\infty} f\left(x',t\right) G_{\Delta}\left(x-x'\right) dx'$ [4] and $\bar{f}(x,t)$ is the resolved mean (filtered variable), $f\left(x',t\right)$ is the non-filtered variable and G_{Δ} is the low-pass spatial filter function.

*Corresponding V. Stetsyuk: v.stetsyuk@hud.ac.uk

Therefore, in LES any instantaneous flow variable can be decomposed into a spatially filtered component (the resolved field) and the fluctuations around the filtered component [5]. The fluctuations around the filtered component are known as the subgrid scale (SGS). In order to couple the detailed chemistry and the computed flow field, (e.g. modelling combustion of diesel fuel) laminar flamelet approach can be used due to its relative simplicity and fast computational time. The laminar flamelet approach considers turbulent non-premixed flames as en ensemble of thin and locally one-dimensional flamelets, which are embedded into the turbulent flow field [2]. In the laminar flamelet approach the chemistry is linked to a single parameter, which is the mixture fraction. In addition to three momentum equations and the continuity equation, a transport equation for the mixture fraction is solved and individual transport equations for reacting species are not considered. Then all reacting species as well as temperature can be linked to a single variable only, which is the mixture fraction that is obtained by the solution of the corresponding transport equation. The dependent (on mixture fraction) variables can be computed prior to flow calculations and stored in the so-called look-up tables, which are known as the flamelet solutions. Since in the LES, only filtered values of the mixture fraction (resolved) are known, the direct mapping from the resolved mixture fraction to the flamelet solution is not possible if subgrid mixture fraction distribution is unknown. In order to embed locally one-dimensional laminar flamelets into the turbulent flow, a concept of filtered density function (FDF) is used. If the shape of the FDF is known, the look-up flamelet tables can then be integrated and all filtered dependent variables can be computed. The FDF can be obtained by solving the transport equation for the FDF or by presuming the shape of the FDF [6]. The shape of the presumed FDF is usually assumed to follow the βfunction probability distribution and parametrized by the first two statistical moments of the mixture fraction, namely, the filtered mixture fraction (the resolved mean) and the 'subgrid' scale mixture fraction variance. The validity and applicability of the βfunction approximation were investigated by using direct numerical simulation (DNS) data of non-premixed reacting flows and it was shown that the βfunction provides a good estimate for the 'true' FDF of the mixture fraction [7]. However, it was shown that the 'true' FDF could substantially deviate from assumed $\beta-$function probability distribution in flow locations containing segregated mixture fraction field with large SGS variance [8], [9]. In addition to the $\beta-$function, the top-hat function can also be used as assumed shape for the FDF [10]. In the context of LES, the $\beta-$function and the top-hat function are defined as follows:

$$\begin{aligned} B_z\left(z,\bar{z},\overline{z''^2}\right) &= \frac{z^{a-1}(1-z)^{b-1}}{\int_0^1 z^{a-1}(1-z)^{b-1}dz} \\ a = \bar{z}\left(\frac{\bar{z}(1-\bar{z})}{\overline{z''^2}}-1\right); b &= (1-\bar{z})\left(\frac{\bar{z}(1-\bar{z})}{\overline{z''^2}}-1\right) \end{aligned} \tag{1}$$

$$\begin{aligned} \Pi_z\left(z,\bar{z},z''^2\right) &= \frac{1}{z_b-z_a} \\ z_b = \bar{z}-\frac{l}{2}; z_a &= \bar{z}+\frac{l}{2}; l = \sqrt{12\overline{z''^2}} \end{aligned} \tag{2}$$

where $\bar{z}$ is the resolved mean (mixture fraction), z is the non-filtered mixture fraction and $\overline{z''^2}$ is the SGS variance, $B_z\left(z,\bar{z},\overline{z''^2}\right)$ is the the presumed $\beta-$FDF, $\Pi_z\left(z,\bar{z},z''^2\right)$ is the presumed top-hat FDF.

If the shape of FDFs are known, the spatially averaged quantities (resolved mean) from the laminar flamelet solutions can be computed directly by an integration with given filtered density function as.

$$\bar{\Phi}(x,y,t) = \int_0^1 \Phi(z) f_z\left(z,\bar{z},\overline{z''^2}\right) dz \tag{3}$$

where $\phi(z)$ is the variable from the laminar flamelet solution (temperature, species mass fraction and etc.), $\bar{\phi}(x,y,t)$ is the resolved variable, $f_z\left(z,\bar{z},z''^2\right)$ can be either the presumed $\beta-$FDF or the presumed top-hat FDF.

The FDF, is in fact the probability density function of a subfilter state that characterises the distribution of the mixture fraction within the confines of the filter. The shape of the FDF can be computed from experimentally measured mixture fraction values as follows: At a given spatial location, a box filter of known size is applied and the mixture fraction values are extracted from the filter confines. The mixture fraction values are then distributed into a number of bins, which are converted into the FDF by counting frequencies in each bin and dividing by a relative bin width (bin width times the number of elements in the dataset). The SGS scalar variance can also be directly computed from the experimentally measured mixture fraction values as.

$$\begin{aligned} \bar{z} &= \tfrac{1}{\Delta^2} \sum_{i=1}^{\Delta^2} z_i \\ \overline{z''^2} &= \tfrac{1}{\Delta^2} \sum_{i=1}^{\Delta^2} (z - \bar{z})^2 \end{aligned} \tag{4}$$

Even though several experimental attempts to measure filtered density function of mixture fraction in both reacting and non-reacting flows exist [8], [12], [13] the measurements and assessment of FDF in swirling flows are almost non-existent. In this research, we analyse the properties of β-function probability distributions, top-hat FDF and comparing those with the measured FDF (true FDF). The FDFs are analysed as a function of degree of mixing and positions in the flow. This research is an extension of previously published research dedicated to the FDF dynamics in swirling flows [14].

2. EXPERIMENTAL SETUP

The flow section (Fig. 1) consisted of two concentric pipes with the annulus supplying swirling air and the central pipe delivering air seeded with acetone vapour (measured scalar quantity). The central pipe (fuel) had an inner diameter D_f of 15 mm and an outer diameter of 18 mm, was 0.75 m long, and was located concentrically in the outer pipe of inner diameter, D of 50.8 mm and centred within it by three screws at 25 mm upstream of the burner exit. The flow development section was 0.264 m long. The annular air stream was split into two separately metered streams named 'swirling' and 'axial' air (Fig. 1). The swirling stream was created by passing air through a static swirler containing 6 milled tangential slots to impart angular momentum. The static swirler was installed in a plenum chamber in which the swirling air was combined with the second stream that delivered the 'axial' air. The detailed description of experimental setup and planar laser-induced fluorescence can be found elsewhere, e.g. [14], [16]. In this research, the swirl number was defined as.

$$\begin{aligned} S &= \tfrac{2G_\Theta}{G_z D} \\ G_\Theta &= 2\pi\rho \int_{r=r_i}^{R} WrUrdr \\ G_x &= 2\pi\rho \int_{r=r_i}^{R} UUrdr \end{aligned} \tag{5}$$

where S is the flow swirl number, G_Θ is the axial flux of angular momentum, G_x is the axial flux of axial momentum, W is the tangential velocity component, U is the axial velocity component, R is the radius of the outer pipe, r_i is the radius of the inner pipe and ρ is the density.

3. RESULTS AND DISCUSSIONS

Figure 2-4 show measured instantaneous mixture fraction (with resolution equal to Batchelor scale of ≈300 μm) spatial distributions at different axial distances for annular swirl number of 0.3, 0.58 and 1.07. Note that instantaneous mixture fraction distributions at different downstream positions were obtained from different

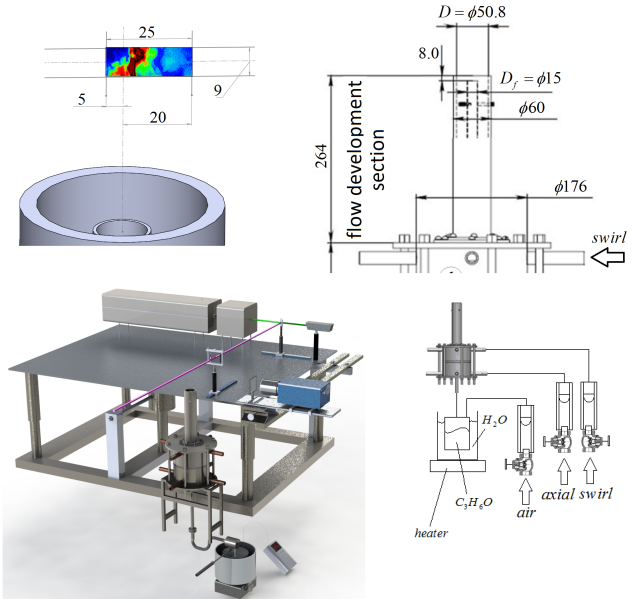

Fig. 1 Experimental configuration and arrangement of coaxial jets (top) and a 3D model of an optical arrangement used to measure spatial distribution of mixture fraction (bottom)

realisations and were not temporally correlated. It is clearly seen that instantaneous mixture fraction spatial distributions are significantly affected by the swirl number. At lower downstream locations and low swirl numbers, segregated mixture fraction fields are observed. As the swirl number increases, faster mixing in the near burner region results in almost homogeneous spatial distributions of the mixture fraction, especially at higher distances from the burner exit. Figure 5 shows an example of segregated mixture fraction field with resolution equal to the Batchelor scale (the first top left image) and the resolved mean for a range of spatial filter sizes. In addition, corresponding SGS scalar variance is shown for each filter size. The resolved mean was obtained by convolution of original mixture fraction field with a filter in spatial domain (discrete convolution). The filter was the box filter of various sizes. In this sense, the resolved mixture fraction field can be seen as the smoothed version of the original mixture fraction field. It can be seen that both, the magnitude and the spatial distributions of the SGS scalar variance are significantly affected by the box filter size. Therefore, it is expected the shape of the presumed FDF will be a strong function of the LES filter size as well as the local mixing regime. Since, the resolved mean is affectively the moving average, the amount of details that can be seen in the resolved mean LES solution (or experimental data) is a function not only the LES filter size but also a function of the local mixing regime. For instance, in the flow regions in which the distribution of mixture fraction is almost homogeneous, i.e. at higher axial distances from the burner exit and sufficiently high swirl numbers, the resolved mean and the original mixture fraction field will be very similar. This is due to the fact that the moving average of mixture fraction values, which are very close to zero (homogeneous mixing) will be close to the original nearly zero values of the mixture fraction field (average of zero is zero). The same behaviour can also be observed in, e.g. regions where mixture fraction values are nearly uniformly distributed, i.e. in the fuel stream close to the burner exit. Therefore, the discrepancy between the original field and the resolved one is solely linked to the level of mixture fraction segregation within the filter confines. It can be suggested that the LES filter (or grid size) can become large in the regions of homogeneous distribution of flow variables. Since, the spatial distributions of the mixture fraction are linked to the spatial distributions of the velocity (scalar is advected by the velocity field), the LES filter size must be smaller, and perhaps comparable to the Batchelor scale, in the regions of steep gradients, e.g. shear layers, recirculating streams, vortices and etc.

Figure 4 shows measured FDF (true), presumed β-FDF and presumed top-hat FDF for two SGS variances,

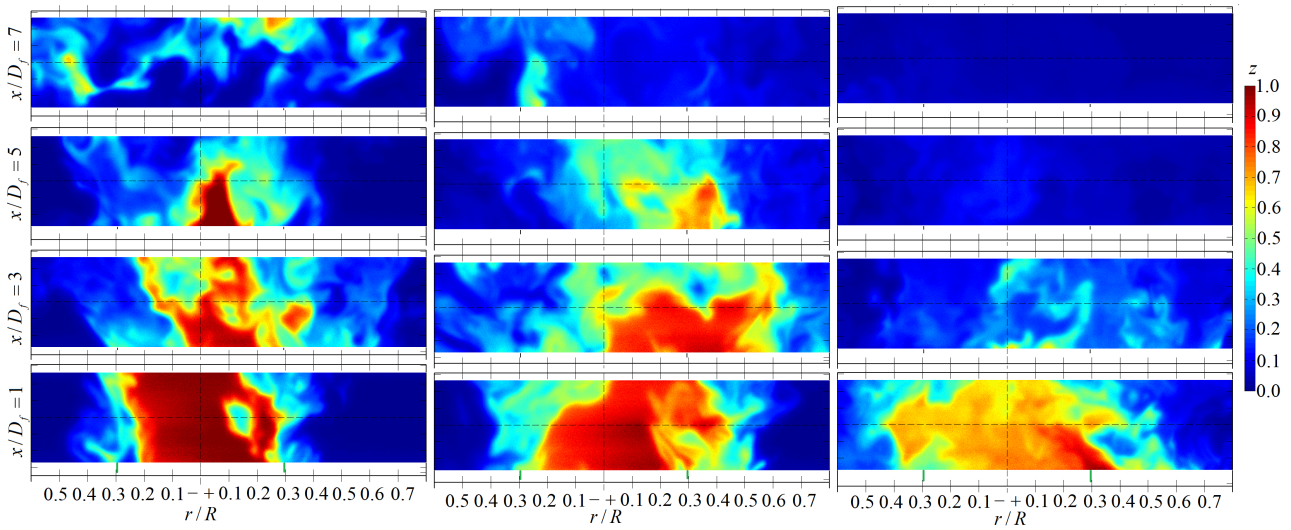

Fig. 2 An example of measured instantaneous mixture fraction distribution at x/D_f=1-7 for annular swirl number S =0.3 (left), 0.58 (middle) and 1.07 (right). Radial scale was normalised by burner radius R =25.4 mm. The position of the edges of the central pipe delivering the acetone vapour jet is shown by the vertical short green lines at $r/R \approx \pm 0.3$. Note that instantaneous mixture fraction distributions at different downstream positions were obtained from different realisations and are not temporally correlated.

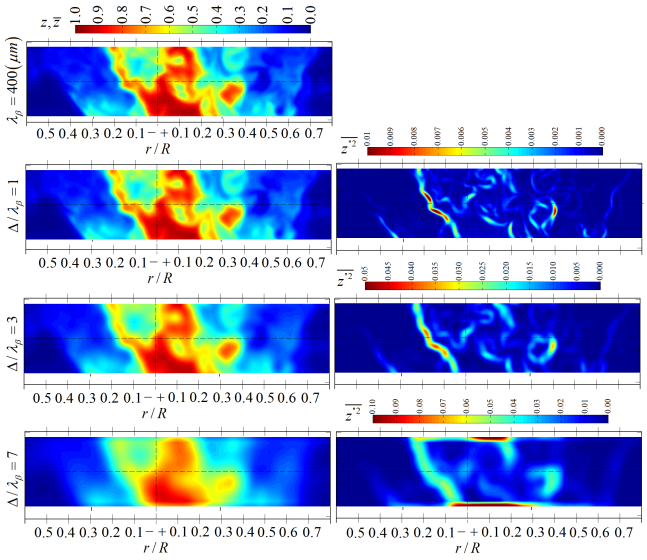

Fig. 3 Measured mixture fraction spatial distribution with resolution equal to the Batchelor scale (the first top left image) and resolved mean for a range of spatial filter sizes. The right column shows corresponding SGS scalar variance.

i.e. relatively small and relatively large for the same LES filter to the Batchelor scale ratio. Note that different SGS variance was obtained from the same filter size but for different LES filter positions in the flow, which are shown as solid black rectangle. As it can be seen for relatively low SGS variance, the β-FDF flows the shape of the true FDF, while for large SGS variance values, the shape of the presumed β-FDF cannot adequately describe the shape of the true FDF. The true FDF exhibits bi-modal behaviour with two distinctive peaks. It was previously mentioned that this bi-modality, which cannot be captured by the presumed β-FDF as well as

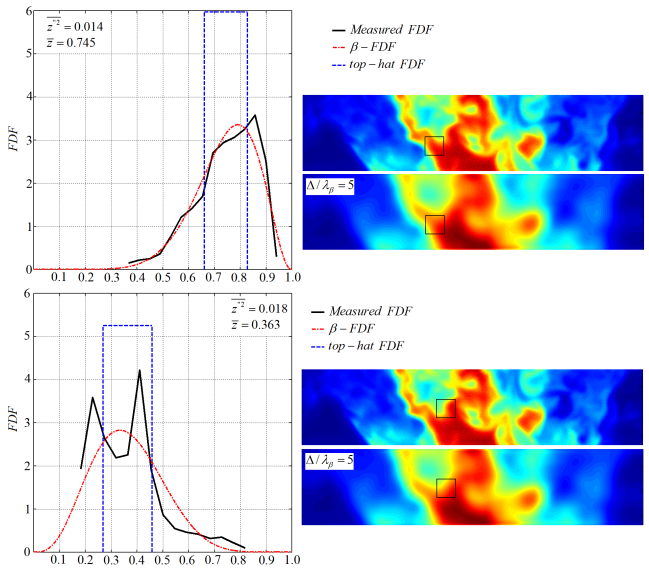

Fig. 4 Measured FDF (true FDF), presumed β-FDF and presumed top-hat FDF for two low and high SGS variances.

by the top-hat FDF may not automatically result in error in the integration of the laminar flamelet solutions [14]. Depending on the actual subfilter mixture fraction distribution, the resulting true FDF can be unimodal and bi-modal. In order to assess the level of discrepancy between presumed FDF and the true one, the measured instantaneous mixture fraction distribution were used in the computation of the resolved temperature distributions by integration of laminar flamelet solution. Due to the length limitations of this article, the reader is referred to [14] for detailed explanations and laminar flamelet solution computational details. First, the 'true' temperature was computed from the mixture fraction values before filtering and then was spatially averaged by the same filter, which was used in the construction of presumed β-FDF as well as the top-hat FDF in order to obtain the resolved temperature. Next, the presumed FDFs were constructed from the mixture fraction resolved mean and from the measured SGS variance (true variance) and laminar flamelet solution was integrated by the presumed FDFs. Note that the temperature, which was obtained from the instantaneous mixture fraction distributions before spatial averaging and spatially averaged later was denoted as the true resolved temperature. Figure 5 shows computed true resolved temperature and the temperature computed by using the presumed β-FDF and the top-hat functions for a range of LES filter sizes normalised by the Batchelor scale (400 μm). Note that the integration was performed only for SGS variance values greater than predefined SGS variance. This is due to the fact that for very small SGS variances ($\leq$0.005), the corresponding FDF will degenerate into delta function. In this case, the computation of resolved temperature and species mass/mole fraction is simply $\overline{T(z)} = T(\bar{z})$. It is seen that for LES filter sizes comparable to the local Batchelor scale, the true resolved temperature and the one predicted by the presumed FDF methods is in good agreement. Slight deviations from the linear relationship can be linked to the local variations in the Batchelor scale or to the errors, which are always present in the experimental data. It is obvious that when the ratio of the LES filter to the local Batchelor scale increases, the corresponding SGS variance increases as well. For large SGS variance, the corresponding FDF can become bi-modal. However this bi-modality does not automatically result in large errors in the integration of the laminar flamelet solution. This is evident from Fig. 5 when analysing the data for larger Δ/λ_β. The discrepancy between true resolved temperature and the one computed by $\beta-$FDF and top-hat FDF is apparent and increases for larger Δ/λ_β. However, for the same true resolved temperature, the values of the corresponding resolved temperature (integrated one) can be different and hence, the error in the temperature prediction is a strong function of local mixing (SGS variance) and the numerical grid size. It is also interesting to note that resolved temperature, which is obtained by the integration of laminar flamelet solution by presumed β-FDF

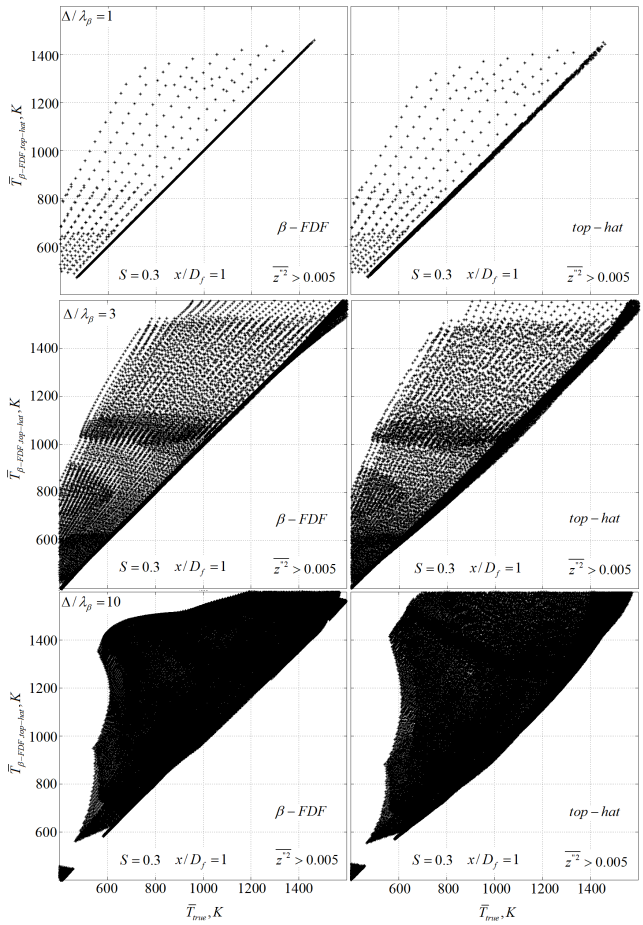

Fig. 5 True resolved temperature (horizontal axis) computed from instantaneous mixture fraction (before filtering) and resolved temperature obtained by integration of laminar flamelet solution (vertical axis) with presumed $\beta-$FDF and top-hat FDF for a range of Δ/β_λ ratios. Left column corresponds to the integration of laminar flamelet solution by $\beta-$FDF, while right column corresponds to the integration of laminar flamelet solution by top-hat FDF.

and top-hat FDF will always be higher than the true resolved temperature.

4. CONCLUSIONS

This research was aimed at analysing the properties of presumed filtered density functions ($\beta-$FDF, top-hat FDF) in the context of LES of reacting non-premixed flows. The FDFs were analysed as a function of flow swirl number, spatial locations in the flow and were linked to the measured subgrid scale variance. The associated laminar flamelet solution integration errors were evaluated for a range of LES filter sizes, which are linked to the numerical grid size. It was experimentally found that the FDFs is unimodal when SGS variance is low and corresponding presumed FDFs will degenerate into delta function. Experimentally measured FDF was found to be bi-modal for large values of SGS variance. It was demonstrated that bimodality does not automatically result in large errors in resolved variables when top-hat FDF or $\beta-$FDF formulations were used. For SGS variances $\leq$0.005, the corresponding measured FDF will degenerate into delta function in which the computation of resolved temperature and species mass/mole fraction does not require the integration of the laminar flamelet solution, i.e. $\overline{T(z)}$. It was experimentally found that resolved temperature obtained by using presumed FDF formulation would always be over-predicted. The error in resolved temperature prediction can be minimised if

and only if the ratio of LES filter size to the local Batchelor scale is equal to 1, i.e. $\Delta/\beta_\lambda = 1$ for segregated mixture fraction fields. However, if well-mixed regime is observed, e.g. large swirl numbers and large axial distances from the burner exit, the ratio of Δ/β_λ can be larger than 1. The only parameter that can quantify the possible errors in the integration of the laminar flamelet solutions is, therefore, linked to the SGS variance and indirectly to the local Batchelor scale.

ACKNOWLEDGMENTS

This work was supported in part by the Alan Howard scholarship for Energy Futures to the first author.

REFERENCES

[1] C. Pera, J. Reveillon, L. Vervisch, P. Domingo, "Modeling subgrid scale mixture fraction variance in LES of evaporating spray," Comb. and Flame 146, 635 (2006).

[2] R. Borghi and P. Moreau, "Turbulent combustion in a premixed flow," Acta Astronautica 4, 321 (1977).

[3] V. Raman, H. Pitsch and R. O. Fox, "Hybrid large eddy simulation/Lagrangian filtered density function approach for simulating turbulent combustion," Combustion and Flame 143, 56 (2005).

[4] C. Pera, J. Reveillon, L.Vervisch, and P. Domingo, "Modeling subgrid scale mixture fraction variance in LES of evaporatingspray," Comb. and Flame 146, 635 (2006).

[5] D. C. Haworth, "Progress in probability density function methods for turbulent reacting flows," Prog. Energy Combust. Sci. 36, 168 (2010).

[6] P. Givi, "Model-free simulations of turbulent reactive flows, Prog. Energy Combust. Sci. 15(1), 1 (1989).

[7] J. Floyd, A. M. Kempf, A. Kronenburg, and R. H. Ram, "A simple model for the filtered density function for passive scalarcombustion LES," Combustion Theory and Modelling 13(4), 559 (2009).

[8] C. Tong, "Measurements of conserved scalar filtered density function in a turbulent jet," Phys. of Fluids 13, 2923 (2001).

[9] D. Wang and C. Tong, "Experimental study of velocity-scalar filtered joint density function for LES of turbulent combustion," Proc. of the Combustion Institute 30(1), 567 (2005).

[10] R. Borghi and P. Moreau, "Turbulent combustion in a premixed flow," Acta Astronautica 4, 321 (1977).

[12] T. G. Drozda, G. Wang, V. Sankaran, J. R. Mayo, J. C. Oefelein, and R. S. Barlow, "Scalar filtered mass density functions in nonpremixed turbulent jet flames Comb. and Flame 155, 54 (2008).

[13] A. G. Rajagopalan and C. Tong, "Experimental investigation of scalar-scalar dissipation filtered joint density function and its transport equation," Phys. of Fluids 15, 227 (2003).

[14] V. Stetsyuk, N. Soulopoulos, Y. Hardalupas, and A. M. K. P. Taylor, "Experimental assessment of presumed filtered density function models," Phys. of Fluids 27, 065107 (2015).

[15] V. D. Milosavljevic, *Natural gas, kerosene and pulverized fuel fired swirl burners*, Ph.D. thesis, Imperial College of Science Technology and Medicine, Department of Mechanical Engineering, 1993.

[16] V. Stetsyuk, N. Soulopoulos, Y. Hardalupas, and A. M. K. P. Taylor, "Scalar dissipation rate statistics in turbulent swirling jets" Phys. of Fluids 28, 075104 (2016).